

Thickness Dependent Structural, Optical, Electrical and Gas Sensing properties of ZnO thin film

Rajarshi Krishna Nath, Subhash Debnath, Indira Dey

Gurucharan University, Silchar, Assam India

DOI: <https://dx.doi.org/10.51584/IJRIAS.2025.1010000097>

Received: 24 October 2025; Accepted: 30 October 2025; Published: 11 November 2025

ABSTRACT

A spray pyrolysis technique have been used to fabricate Zinc Oxide (ZnO) thin films using $\text{Zn}(\text{CH}_3\text{COO})_2$ as a precursor solution. The structural, optical and electrical properties of the films are explored and then tested for ethanol sensing. Structural studies show that the films are polycrystalline in nature, possessing “hexagonal wurtzite” structure. A decrease of FWHM(Full Width at Half Maximum) with an increase in film thickness is observed, which confirms the increase of crystallite size with an increase in film thickness. The optical band gap of the films was studied and a “Blue Shift” was observed from 2.97eV to 3.12eV as the film thickness was decreased from 441nm to 172nm. The crystallite sizes obtained from XRD and TEM studies shows an increase with a increase in film thickness. The gas sensing properties of the films have been studied using ethanol, methanol, acetone and LPG at different concentrations and at different operating temperatures. It is observed that thinner films show higher response for all the test gas/vapours.

Keywords: ZnO thin films, spray pyrolysis, blue shift, gas sensing.

INTRODUCTION

Zinc oxide (ZnO) is one of the most prominent metal- oxide n-type semiconductors of hexagonal (wurtzite) structure with a direct band gap of about 3.37eV at room temperature. Because of its good electrical and optical properties, thermal/chemical stability, abundance in nature, low cost and absence of toxicity, this material has got wide applications in electronic and optoelectronic devices such as transparent conductors, solar cell windows, gas sensors etc.[1-6]. For gas sensing purposes, this material has been investigated in various forms such as single crystals, sintered pellets, thick films, thin films and heterojunctions [7-12]. However, thin films are more suitable for such sensors because gas sensing properties are related to the material surface where the gases are adsorbed and the surface reactions occur. This reaction modifies the concentration of charge carriers in the material giving rise to a change in its electrical resistance, which is used for the purpose of gas detection. In addition, solid state thin film gas sensors offer certain advantages compared to sintered pellets or thick film sensors, i.e their fabrication process is compatible with microelectronic fabrication processes. In this paper, we report a study on thickness dependent structural, optical, electrical and gas sensing properties of ZnO thin films prepared by chemical spray pyrolysis technique.

Experimental Details.

ZnO thin films are deposited on to the glass substrates, which are cleaned with freshly prepared chromic acid, detergent solution and distilled water. The schematic representation of the spray system is described elsewhere [13]. The deposition method involves the decomposition of a solution of 0.1 M concentration of high purity zinc acetate dehydrate (Merck, India) prepared in distilled water. The resulting solution is subsequently sprayed onto heated substrate at a constant temperature of $(410 \pm 20^\circ\text{C})$, which is monitored by a chromel alumel thermocouple fitted close to the substrate with the help of a Motwane Digital Multimeter (Model: 454). The atomization of the solution into a spray of fine droplets is affected by the spray nozzle with the help of compressed air as carrier gas.

The thickness of the films is determined by the weight difference method using an electronic precision balance (Citizen, model: CY 204). Structural analysis of the films is carried out using a PANalytical X'Pert Pro X-ray diffractometer with $\text{CuK}\alpha$ radiation ($\lambda = 1.5418 \text{ \AA}$) as an X-ray source at 40kV and 30mA in the scanning angle

(2 θ) from 30 to 70 $^{\circ}$ with a scan speed 0.02 $^{\circ}$ / s. The optical transmission spectra of the films are obtained in the UV/VIS/near IR region up to 1100 nm using Perkin Elmer UV-VIS spectrometer (Model: Lamda 35). For making ohmic contacts at both the ends of the film, high conducting silver paste is used and is dried at a temperature of 150 $^{\circ}$ C. The film is mounted on a homemade two-probe assembly placed inside a silica tube, which is inserted co-axially inside a resistance-heated furnace. The electrical resistance of the film is measured before and after exposure to ethanol using a Keithly System Electrometer (Model: 6514)

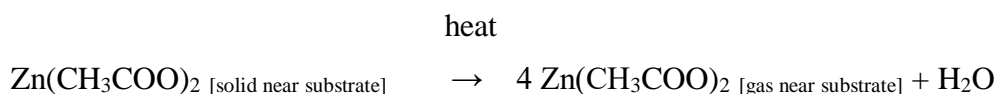
Table 1. Process parameters for the deposition of ZnO thin films.

Spray parameters	Optimum value/ Item
Nozzle	Glass
Nozzle- Substrate distance	50 cm
Solution concentration	0.1 M
Solvent	Distilled water
Solution flow rate	5 ml/ min
Carrier gas	Compressed air
Gas pressure	2.8 kg / cm 2
Substrate temperature	(410 \pm 20) $^{\circ}$ C
Angle of spraying	30- 45 $^{\circ}$

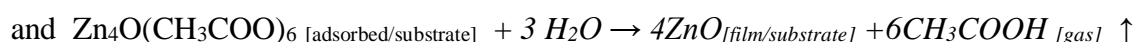
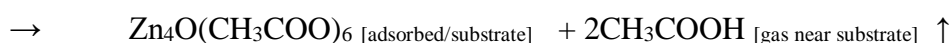
RESULTS AND DISCUSSION

Formation of Zinc oxide (ZnO) thin film

When aerosol droplets arrive close to the heated glass substrates, a pyrolytic (endothermic) process takes place and a highly adherent film is formed on the glass substrates. Possible reaction mechanism in ZnO film formation is as follows. [14]



Adsorption



Structural analysis

The X-ray diffractograms of ZnO films of two different thicknesses namely (172 \pm 14) nm and (225 \pm 18) nm is shown in fig. 1.

Fig.1. XRD patterns of ZnO film of two different thickness.

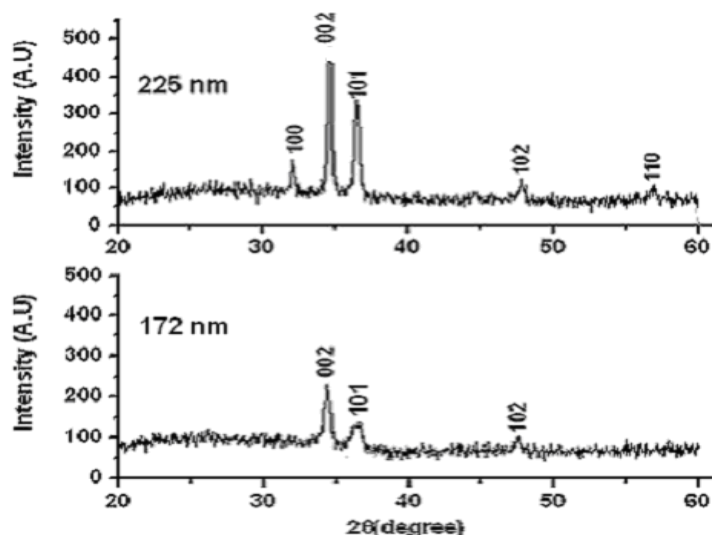


Table 2.shows the different XRD data obtained for the two films.

Film thickness (nm)	Diffraction planes (hkl)	Intensity (A.U)	Diffraction angle,2 θ (deg)	Average crystallite Size(nm)	Lattice Strain (%)
172 \pm 14	002	231	34.4	41.69 \pm 0.36	0.28
	101	141	36.25		
	102	103	47.5		
225 \pm 18	100	178	32	48.72 \pm 0.42	0.23
	002	475	34.6		
	101	334	36.45		
	102	124	47.75		
	110	109	56.85		

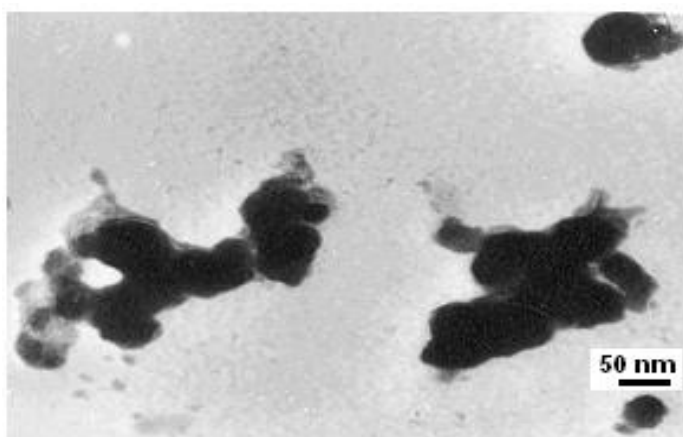
GIXRD data of ZnO film of two different thickness viz.172 nm and 225 nm

It is observed from the fig.1 that the intensity of the peak increases due to an increase in film thickness. Further a decrease of FWHM with an increase in film thickness is observed, which confirms the increase of crystallite size with an increase in film thickness as reported by other [15]. Since the peak intensity and grain size are associated with the crystallinity of the film, poor crystallinity in a thinner film could be associated with the incomplete growth of the crystallites as only few atomic layers of disordered atoms constitute the bulk of the film [15].

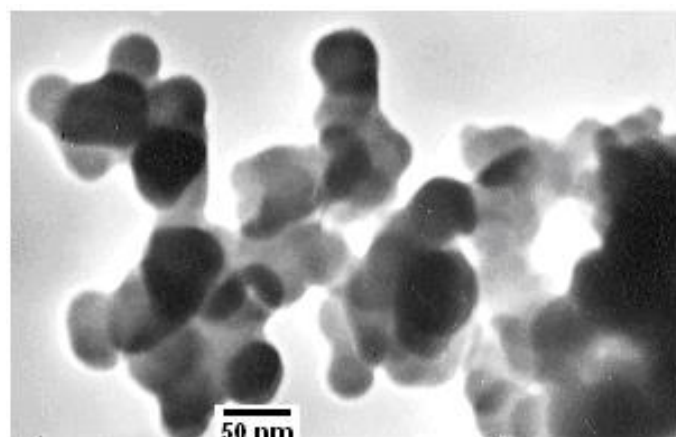
Transmission Electron Microscopic studies

The TEM images of ZnO thin film of two different thicknesses are displayed below

Fig.2. TEM images of ZnO



Film thickness: 172 nm



Film thickness: 225 nm

The crystallite size obtained from TEM for the two ZnO films of thicknesses 172 nm and 225 nm are listed in table 3.

Table 3. Crystallite size from TEM

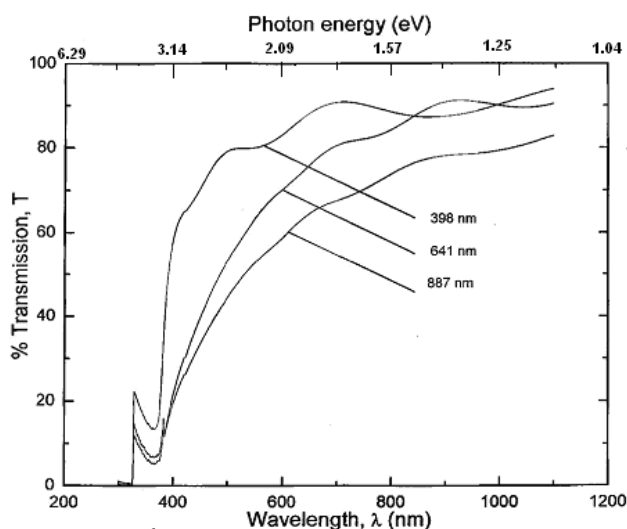
Film thickness (nm)	Crystallite size (nm)
172 \pm 14	42.5
225 \pm 18	49.8

It is observed that the crystallite sizes obtained by XRD and TEM for the two films are quite similar. Both the XRD and TEM studies reveal that the crystallite size decreases with a decrease in film thickness.

Optical Studies

The optical transmission spectra of zinc oxide (ZnO) thin films of different thicknesses are shown in fig.3.

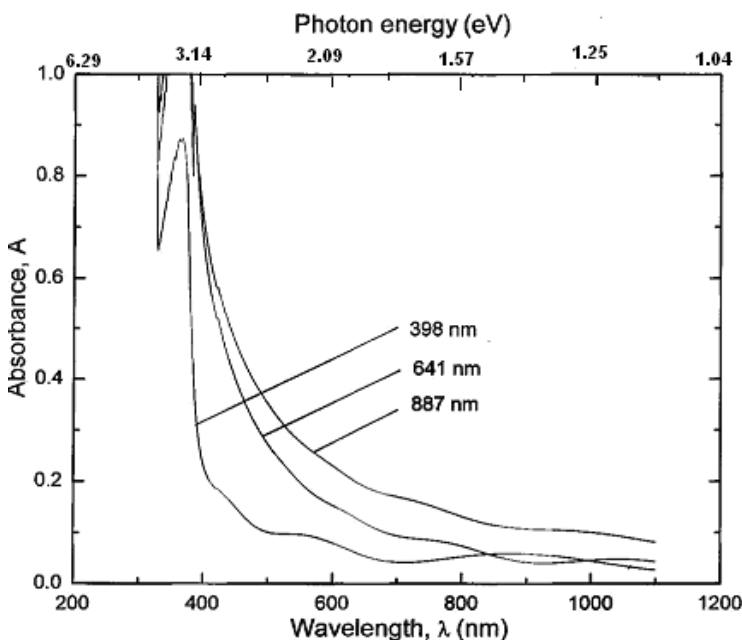
Fig.3. Optical transmission spectra of ZnO films of different thickness



These spectra show that for film having 398 nm thickness, the average transmission over the range 500-1100 nm exceeds 80 % with a sharp fall near the fundamental absorption; whereas fall in transmission is gradual for the other films.

The optical absorbance spectra of the films are shown in figure 4.

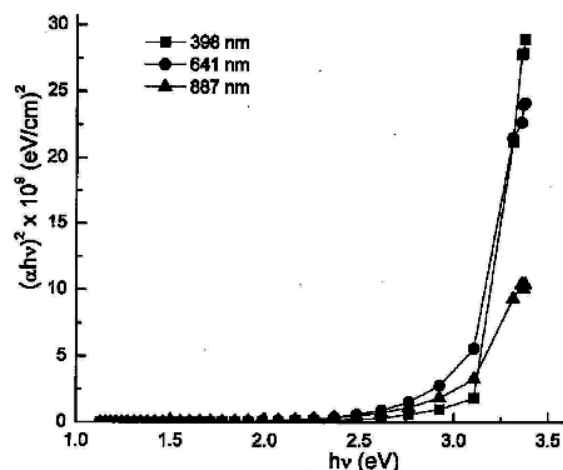
Fig.4. Absorbance spectra of ZnO thin films of different thickness.



These spectra reveal that films grown under the same parametric conditions have low absorbance in the visible/ near infrared region while absorbance is high in the ultraviolet region. The absorption coefficient (α) was found to follow the relation [13].

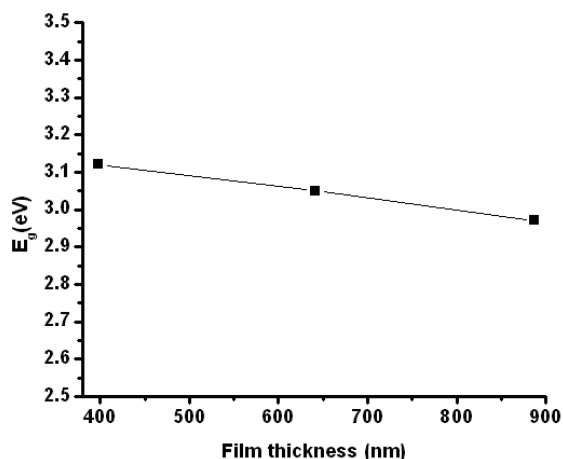
Plots of $(\alpha h\nu)^2$ versus photon energy ($h\nu$) in the absorption region near the fundamental absorption edge is shown in figure.5. In this case $n = 2$ gives the best linear graph which indicates direct allowed transition in the film material as mentioned earlier.

Fig.5. Plots of $(\alpha h\nu)^2$ vs $h\nu$ for the ZnO films of different thicknesses.



The optical energy gap, estimated from the extrapolation of the linear portion of the graph to the photon energy axis, and its dependence on film thickness is illustrated in figure.6.

Fig.6. Optical energy gap Vs thickness of the film.



It is observed that optical band gap (E_g) decreases with increasing film thickness. This may be due to the structural defects in the films arisen during the time of their preparation, which could give rise to the allowed states near the conduction band in the energy band gap [13]. In case of much thicker films, these allowed states could well merge with the conduction band resulting in the reduction of the energy band gap.

The variation of band gap with film thickness is listed in table 4.

Table 4. Variation of band gap with film thickness

Film thickness (nm)	Optical band gap (eV)
398 ± 15	3.12 ± 0.01
641 ± 17	3.05 ± 0.01
887 ± 21	2.97 ± 0.01

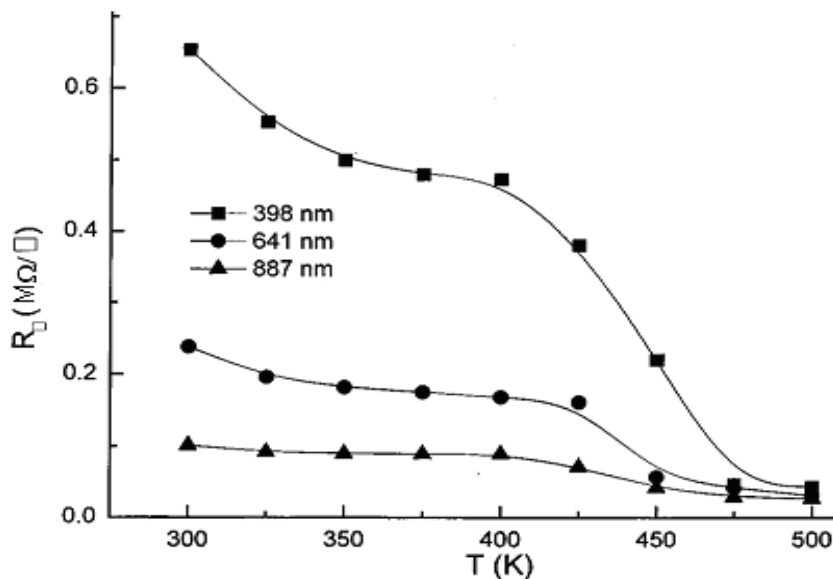
The decreasing band gap with increasing thickness indicates a decrease in barrier height with an increase in crystallite size [16].

Electrical studies

The electrical resistance, in order of $M\Omega$, observed for our ZnO films at room temperature (300 K) can be attributed to the large density of extrinsic traps at the grain boundaries due to oxygen chemisorption. These traps

deplete the grains and result in a charge carrier barrier at the grain boundaries [17]. This effect can be more relevant for small grain size. The variations in sheet resistance (R_{\square} , expressed in $M\Omega/\square$) of the ZnO thin films with temperature is shown in fig.7.

Fig.7. Variations in sheet resistance of the ZnO thin films with temperature.



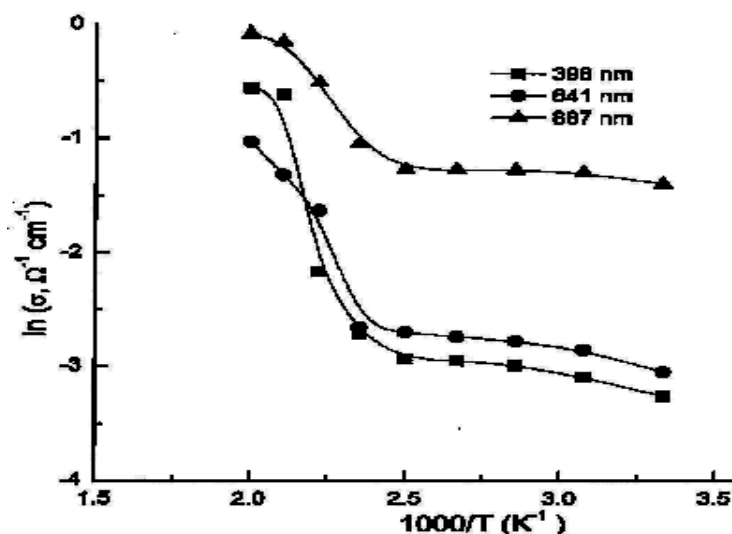
For all the films, the sheet resistance is found to decrease with increasing temperature as well as film thickness in the temperature range 300-500 K. The decrease in resistance is related to the increase in carrier concentration resulting from activation of deep and shallow donors which may arise due to native defects such as interstitial zinc atoms and oxygen vacancies [18].

The inverse absolute temperature dependence of the electrical conductivity of the films is shown in fig.3.16. The activation energy was obtained using the relation [13].

$$\sigma = \sigma_0 \exp(-E/kT)$$

where σ is the electrical conductivity at any temperature, σ_0 a constant, E the activation energy for conduction, k the Boltzmann constant and T the absolute temperature

Fig.8. Plot of $\ln \sigma$ vs $1000/T$ for the ZnO films of different thickness



The conductivity studies on films show that all the films exhibit two activation energies at different temperature regions. These activation energies vary with film thickness and are listed in table 5.

Table .5. Variation of activation energy with thickness for ZnO thin films.

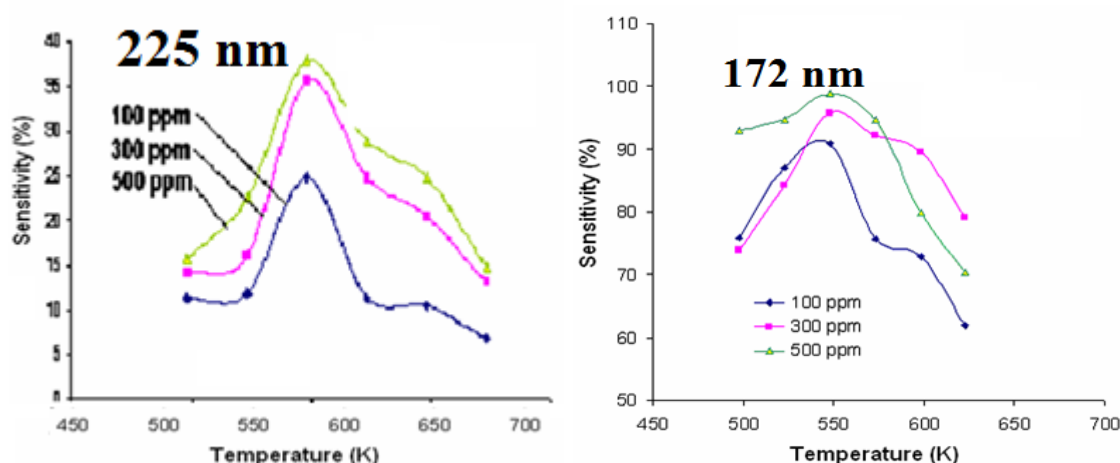
Film thickness (nm)	Activation energy	
	$E_1(\text{eV})[300-400\text{K}]$	$E_2(\text{eV})[400-500\text{K}]$
398 ± 15	0.034	0.468
641 ± 17	0.033	0.323
887 ± 21	0.012	0.226

The results indicate the presence of two donor levels, one deep and one shallow near the bottom of the conduction band. Both of these levels depend on the film thickness, and are found to decrease with increasing thickness [13].

Gas Sensing Properties

The basic principle of semiconductor gas sensors is the change in resistance of the sensor material that arises from the change in electron concentration near the sensor surface by the reaction with gases or vapours. The sensing characteristics of the ZnO thin film of two different thickness viz 225 nm and 172 nm as a function of operating temperature for three different concentrations namely 100 ppm, 300 ppm and 500 ppm of ethanol is shown in fig 9.

Fig. 9. Sensitivity characteristics of ZnO thin film of two different thickness (225 nm and 172 nm) as a function of operating temperature for three different concentrations(100 ppm, 300 ppm and 500 ppm) of ethanol.



It is seen that for concentrations of ethanol in air, the sensitivity of ZnO thin film increases up to 550 K and then decreases with further increase in temperature. It is observed that compared to the film of 225 nm thickness, sensitivity increases highly in case of 172 nm thickness. The maximum sensitivity for 225 nm thickness is found to be ~ 38% where as for 172 nm thickness, it is found to be ~98%. This is attributed to the fact that film of 172 nm thickness has smaller crystallite size than that of 225 nm thickness as observed in case of XRD and TEM studies. As we know, smaller the crystallite size, the larger the specific surface area (S/V), which results in greater oxygen adsorption and higher sensitivity. Similar phenomenon have been observed in case of other tested gases /vapours namely LPG, methanol, acetone etc.

CONCLUSION

A study on the sprayed ZnO thin film has been carried out to investigate the effect of thickness variation on structural, optical, electrical and gas sensing properties. XRD studies show that the films are polycrystalline in nature with a decrease of FWHM with an increase of film thickness, which confirms the increase of crystallite size with an increase in film thickness. The decrease in crystallite size with the decrease in film thickness has also been cross checked by TEM studies. The UV-IS spectroscopic studies reveal that optical band gap (E_g) decreases with an increase in film thickness. It is also observed that the sensitivity of the film towards a particular gas/vapour increases with a decrease in film thickness.

ACKNOWLEDGEMENT

The authors wish to acknowledge Dr. P.P.Sahay, Department of Physics, MNNIT, Allahabad, UP, India for his technical assistance in this work.

REFERENCES

1. Paraguay. F. D., Miki-Yoshida. M., Morales. J., Solis, J., Estrada L.W., Thin Solid Films, vol. 373. pp.137-140. 2000.
2. Sahay. P.P., J.Mater.Sci. vol. 40,pp.4383-4385. 2005.
3. Mitra. P., Maiti. H.S., Sensors and Actuators B, vol. 97. pp. 49-58. 2004.
4. Baruwati. B., Kumar. D.K., Manorama. S.V., Sensors and Actuators B, vol. 119, pp. 676-682. 2006
5. Pizzni. S., Butta. N., Narducci. Palladino. D.M., J. Electrochem. Soc. vol.136, No.7, July 1989.
6. Sahay. P.P., Nath. R.K., Sensors and Actuators B, vol. 133, pp.222-227. 2008.
7. Patel. N.G., Patel. D., Vaishnav. V.S., Sensors and Actuators B, vol.96, pp. 180-189. 2003.
8. Morrison. S.R., Sensors and Actuators, vol. 2, pp.329-341. 1982.
9. Watson. J. Sensors and Actuators, vol. 5. pp. 29-42. 1984.
10. Mitra. P., Chatterjee. A.P., Maiti H.S., Materials Letters, vol. 35, pp. 33-38. 1998.
11. Jones. A., Jones. T.A., Mann. B., Griffith. J.G., Sens.Actuators. vol. 5, pp. 75-88. 1984.
12. Arshak. K., Gaiden. I., Mater. Sci. Eng. B. vol.118. pp. 44-49. 2005.
13. P.P.Sahay, S.Tiwari, R.K.Nath, Cryst.Res.Technol.42, No.7, 723-729 (2007)
14. Sahay P.P., Tiwari S., Nath R.K; Cryst. Res. Technol. Vol.42, No.7, pp.723-729. 2007
15. Jain, A. Sagar P., Mehra R.M., Materials Science-Poland, Vol.25, No.1, 2007.
16. Tyagi P. and Vedeshwar A.G., Bull.Mater. Sci., vol. 24, No. 3, June 2001, pp. 297-3
17. Demiryont H. and Nietering K. E, Sol. Energ. Mat. Vol.9, p.79 1989
18. Kröger F. A., "The Chemistry of Imperfect Crystals", North-Holland, Amsterdam, 1964.